THERMODYNAMIC DESIGN AND EMISSIONS MODEL OF A MACH 1.8 SUPERSONIC AIRLINER ENGINE

Martin Plohr[1], Sebastian Zenkner[1], Sebastian Bake[2], Dirk Zeitz[2]

[1]German Aerospace Center (DLR) Institute of Propulsion Technology, Engine Department, Linder Hoehe, 51147 Koeln, Germany
[2]Rolls-Royce Deutschland Ltd. & Co KG, Eschenweg 11, 15827 Blankenfelde-Mahlow, Germany

Abstract

Keywords: Supersonic Engine, Landing and Take-off Noise, Emissions, Emissions Standards

1. Introduction

The EU-project SENECA aims at improving the understanding and modeling of the environmental impact of new supersonic aircraft. For this purpose, four different aircraft concepts have been developed for detailed assessment. For each of these concepts, individual engine design processes have been created and applied, considering multiple optimization objectives like fuel efficiency, engine lifetime and supersonic drag as well as landing and take-off noise and emissions. One of these concepts is an airliner with a design Mach number of 1.8, for a projected entry into service in the 2025-2035 timeframe. The process of creating an engine model for this concept, including gaseous and nvPM emissions estimations, is described in this paper. An iterative process has been applied for this purpose, during which a preliminary study, an initial and a final engine design have been created. The results of these have each been fed back into the overall SENECA design and modeling cycle and resulted in updated design requirements provided by SENECA's airframe, noise and emissions modeling work packages. The final design has demonstrated the capability to meet all design requirements, however, meeting the current subsonic NOx emissions limits turned out challenging due to the low OPR of the engine cycle.

2. Engine Design

2.1 Design Procedure

The initial design was based on performance requirements provided by the airframe design work package (WP2) of the SENECA project. In addition, noise constraints were provided by the noise modelling work package (WP5). In an initial assessment, it turned out that these constraints and requirements have strong impacts on the engine cycle, sometimes in opposite directions. Therefore, as a first step a parametric study on supersonic engine cycle design has been performed. The results of this study have guided the subsequent iterative optimization process.

At the same time, technology assumptions for an expected entry into service date in the 2025-2035 timeframe to be applied in this process have been derived from a literature study and discussed and agreed with project partners.

In order to be able to provide basic engine geometrical and weight information to the SENECA partners, a simplified engine geometry was subsequently created by a knowledge-based sketching process.

2.2 Technology Assumptions

For the determination of technology assumptions for the Mach 1.8 airliner engine design, a literature study was performed for a technology horizon according to an entry into service date of 2025 - 2035.

Several potential published sources were identified ([12], [1], [9] and [4]) and average values of all relevant component efficiencies, as well as the operating limits (in particular the maximum turbine inlet temperature and the compressor outlet temperature), were derived from these sources as input for a final internal discussion.

This discussion has revealed an important difference between the design criteria for sub- and supersonic engines: While for a subsonic engine, the highest internal temperatures occur in the take-off and initial climb conditions, for a supersonic engine these will be found in the top of climb and supersonic cruise. This is caused by the deceleration of the inflowing air in the engine intake from supersonic to subsonic speed, resulting in significant pressure and temperature rise. As a consequence, the maximum cycle temperatures of a supersonic engine must be acceptable for continuous operation, while for a subsonic engine they will only prevail for a short time during take-off (usually 5 minutes, as stated in the engine type certificate data sheets). Due to the time-dependent effects of the gas temperatures on oxidation and creep of the blade material, the acceptable maximum gas temperatures for a supersonic engine will therefore be significantly lower than for a subsonic one. The final agreed technology assumptions are summarized in Table 1.

SENECA Ma 1.8 airliner engine technology assumptions, design point	
Fan polytropic efficiency	0.9
Fan inflow Mach number	0.65
Fan hub/tip ratio	0.32
Fan tip speed	520m/s
HP compressor polytropic efficiency	0.91
Max. cont. compressor exit temperature	850K
Combustor efficiency	0.9999
Combustor pressure ratio	0.96
HP turbine isentropic efficiency	0.91 (uncooled)
LP turbine isentropic efficiency	0.92
Mixer pressure ratio	0.985
Mixing efficiency	0.85

Table 1 – Technology assumptions for SENECA MA 1,8 airliner engine design

2.3 Parametric Study on Supersonic Engine Cycle Design

As the basic engine layout, a two-spool, non-afterburning, mixed exhaust turbofan configuration was selected, including a variable convergent-divergent nozzle, where the nozzle exit area is adjustable for low take-off noise and efficient supersonic flight (in a later stage of the design iteration an additional variable throat area was introduced). A thermodynamic cycle model was set up with DLR's gas turbine simulation tool GTlab [11]. The general layout of this model and the internal station numbering are shown in Figure 1.

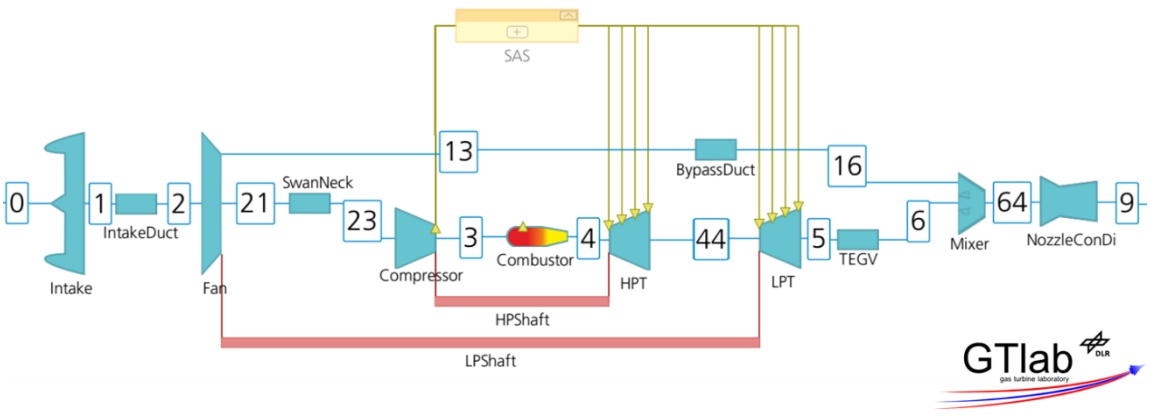

Figure 1 – General engine model layout and internal station numbering

An initial parametric cycle study has been performed with this model to determine the main drivers on the cycle parameters with respect to the design constraints given by SENECA WPs 2 (airframe thrust requirements), 4 (emissions targets) and 5 (noise requirements). No detailed noise modelling has been performed at this early design stage, but a subsonic jet speed was required for the low altitude operating conditions. With these design constraints and a fixed set of component technology assumptions, there is only a limited number of parameters that are free to be varied in an initial thermodynamic engine cycle design study:

- The efficiencies of the compressors and the maximum allowable compressor exit temperature (T3) determine the achievable overall pressure ratio (OPR) of the engine cycle.
- The efficiencies of the turbines, the exhaust mixing conditions and the selected bypass ratio (BPR) determine the fan pressure ratio (FPR)
- The allowed blade metal temperature of the high-pressure turbine (HPT) and the effectiveness of the cooling system determine the maximum turbine inlet temperature (TIT or T41)

OPR, BPR and T41 are the main parameters that determine the engine thermal and propulsion efficiency. With the fixed set of technology assumptions, the BPR is the only remaining free parameter in this set.

Furthermore, the thrust and size (fan diameter) of the engine is determined by the air mass flow through the engine at the design point (DP). For this study, the Top of Climb (ToC) condition was selected as the DP.

Figure 2 shows the effect of a variation of the BPR of the uninstalled engine on the cycle efficiency, represented by the thrust specific fuel consumption (SFC), the fan diameter as a measure of the engine size and the exhaust jet Mach number (Ma9), which is a main driver of the perceived noise from the aircraft in take-off and climb conditions.

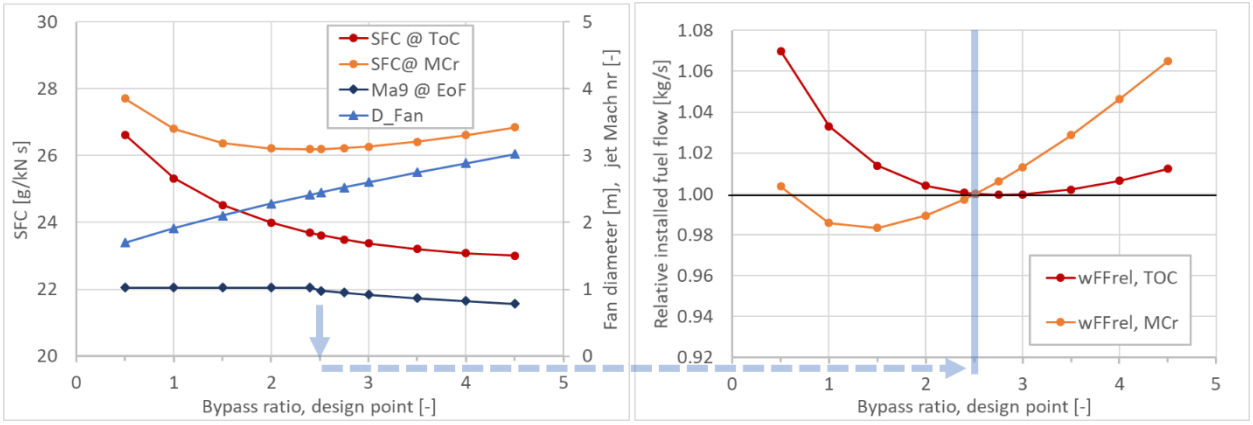

Figure 2 – Results of the initial Task 3.3 engine cycle design study:
Left: SFC at Top of Climb (ToC) and Mid Cruise (MCr), fan diameter (D_Fan) and exhaust jet Mach number (Ma9) as function of the design point BPR for the uninstalled engine
Right: Relative fuel flow (wFFrel) of installed engine, based on simplified installation drag model

From the left diagram, it becomes obvious that the BPR for minimum SFC for the ToC condition is much higher than that for the Mid Cruise (MCr) condition, which is around 2.5. Incidentally, this is also the BPR above which the exhaust jet becomes subsonic at the End of Field operating condition (EoF), assuming the variable nozzle is set to a convergent configuration (Ma9 < 1, blue arrow in the left and blue line in the right diagram). Consequently, for the underlying assumptions of this study, a BPR of slightly above 2.5 would provide both, optimum supersonic cruise fuel efficiency as well as acceptable jet noise in ground proximity. On the other hand, the figure also shows the engine size (D_Fan) is continuously increasing with the design BPR. Particularly in supersonic flight conditions, the engine diameter has a strong impact on the drag of the aircraft, which would in turn increase the

thrust required from the engine to maintain steady cruise flight conditions.

To account for this effect and determine the impact of the BPR on the fuel efficiency of the installed engine, a simplified, initial assumption from a DLR-internal study has been applied. These results are shown in the right diagram of Figure 2.

Obviously, the drag impact of the fan diameter results in a shift of the fuel optimum BPR to significantly lower values. The optimum shifts from BPR>5 to BPR≈2.7 for ToC and from BPR≈2.5 to BPR<1.5 for the MCr condition. However, the jet velocities resulting from such BPR values (see Ma9@EoF in the left diagram of Figure 2), would clearly lead to unacceptable noise levels at take-off and initial climb conditions.

As a result of this initial thermodynamic engine cycle study, it was determined that the noise requirement (subsonic exhaust jet at take-off) will be the limiting factor for the achievable fuel efficiency of the engine, when all other technology parameters are fixed. The optimization loop for the initial design of the first engine model has been set up according to the findings of this study.

2.4 Preliminary Engine Design

The first optimization loop resulted in an engine cycle with OPR 23.4 and a BPR of 3.19 at the design condition (Top of Climb) – slightly higher as found in the parametric study, to avoid choking of the nozzle under certain operating conditions, e.g. at high ambient temperatures. The fuel consumption of this engine was in the range required, however no installation effects had been considered at this stage. An initial emissions estimation (for a detailed description see below) revealed potential to meet current subsonic gaseous emissions limits.

3. Final Optimized Design

3.1 Change in Design Parameters

The preliminary design described above did not include detailed assessment of the thrust-dependent intake and afterbody drag elements in supersonic flight, which may significantly reduce the installed cruise thrust of a supersonic engine. These drag elements have been included in the final optimization process.

Furthermore, the initial assumption of a twin-engine configuration had been changed to a quad engine airliner, to benefit from higher noise limits and potential use of existing core components (i.e. compressor, combustor and turbines), which would not be possible for the twin-engine design due to its very large size, surpassing even the largest core engines in service today.

As a result of these changes, the engine thrust requirements were reduced by a factor of 2. Further changes in these requirements resulted from an adaptation of the initial airliner configuration with the fuel efficiency and weight data resulting from the preliminary engine design data.

Finally, it was found that, although the preliminary engine design had a subsonic exhaust jet at low speeds to limit the take-off noise, this was not sufficient to meet all ICAO Annex 16, Vol. I, Ch.14 noise limits. Therefore, it was decided to add an additional variability to the exhaust system, which would allow to increase the nozzle throat area at low altitude operation, thereby reducing the fan pressure ratio while increasing its mass flow.

The engine design process has been adapted to match these changes. The component efficiency assumptions were modified using mass flow-dependent scaling factors as recommended in [4]. Due to the large size of the components, this scaling effect was only small. The assumed temperature limits and cooling assumptions remained unchanged.

The most important change to the design process was the introduction of the thrust-dependent drag elements. These had a significant impact on the engine installed thrust and it was found that the preliminary design suffered from a mismatch between engine air demand and actual intake flow in supersonic cruise and transonic acceleration. Since an adaptation of the airframe geometry was not possible due to capacity constraints, a new design mission was created, which resulted in a better matching of intake flow and engine air demand throughout the supersonic flight phase.

3.2 Consideration of Intake Drag

The design of an intake for an engine to operate at supersonic speeds is much more complex than for a subsonic engine. To be acceptable to the fan, the incoming supersonic flow must be decelerated to subsonic speed by a system of shocks. In an ideal case, the intake would always deliver exactly the amount of air the engine needs. In reality, that is not possible, because the projected maximum frontal area of the engine is invariable. As a consequence, the intake needs to get rid of varying amounts of excess air, depending on the thrust setting of the engine, by spillage or bypass systems. This spillage or bypass air creates significant additional drag in supersonic flight, the exact amount being dependent on the intake design and the respective flight conditions and engine thrust settings. Drag coefficients of some actual intakes are available in intake drag maps as functions of intake flow area fractions (e.g. [7]). These drag maps have been scaled and interpolated, as appropriate, for the purpose of the engine design optimization for the Ma 1.8 airliner.

3.3 Variable Nozzle Areas

The engine model from the first iteration featured a variable nozzle exit area in order to be able to keep the exhaust flow subsonic in low altitude conditions, while providing optimum expansion of the jet in supersonic flight. However, it appeared that this configuration was not sufficient to reduce the jet speed -and hence engine noise- at certain climb-out conditions. An even larger engine would be required to overcome this issue, which would have detrimental impacts on cruise fuel efficiency.
Therefore, it was decided to consider an additional variable nozzle throat area for the optimized engine design. Opening the nozzle throat at low flight Mach numbers increases the fan mass flow while reducing its pressure ratio. As a result, subsonic flow conditions can be maintained in the nozzle up to higher thrust than with the original configuration, without compromising on cruise performance.
Mach number-dependent schedules as shown in Figure 4 have been implemented to adjust the nozzle areas.

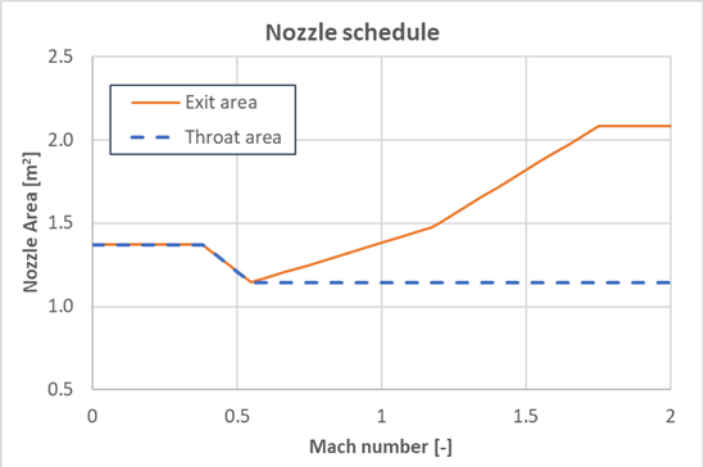

Figure 4 – Mach number-dependent nozzle area schedules

These schedules approximate the nozzle area ratio required for ideal expansion by piecewise linear functions. Additional boundary conditions have been considered, in particular a limitation of the exit area by the maximum engine outer diameter.

3.4 Results for the Final Engine Design

An overview of thermodynamic engine data of the final optimized (quad jet) engine design is shown in Table 2 (right side), compared to the preliminary (twin jet) engine model (see section 2.4) after including installation drag elements (left side).

		Ma 1.8 preliminary engine design					*Ma 1.8 final engine design*				
		Top of Climb	EOF + 15K	Initial TA	Final TA	Mid Cruise	Top of Climb	EOF + 15K	Initial TA	Final TA	Mid Cruise
Altitude	[m]	12496.8	0.0	10668.0	10668.0	14630.4	10668.0	0.0	10668.0	10668.0	15266.2
Mach number	[-]	1.60	0.25	0.90	1.30	1.80	1.54	0.25	0.90	1.30	1.80
Installed net thrust	[N]	133198	266339	111806	65396	69826	81645	133406	44242	64020	39739
Installed SFC	[g/kNs]	25.6	15.0	21.9	50.3	31.3	25.2	17.1	19.7	23.8	27.6
OPR	[-]	24.1	22.8	33.5	27.9	17.5	22.6	21.9	24.3	24.1	17.7
BPR	[-]	3.22	3.35	2.73	3.00	3.8	2.67	3.19	2.60	2.61	2.98
Jet Mach number	[-]	2.00	0.94	1.47	1.74	2.04	1.95	0.97	1.48	1.77	2.10
Corrected fan flow	[kg/s]	987.9	982.9	992.0	948.5	876.1	404.0	440.0	419.6	415.9	362.1
Compressor exit temp.	[K]	850.0	746.6	800.8	826.4	835.2	830.9	798.4	680.9	774.7	849.8
Combustor mass flow, corr.	[kg/s]	12.9	13.1	11.5	11.7	13.1	6.5	6.5	6.5	6.5	6.6
Combustor exit FAR	[-]	0.0264	0.0218	0.0280	0.0272	0.0236	0.0268	0.0260	0.0213	0.0249	0.0261

Table 2 – Thermodynamic engine data of preliminary (left) and final optimized (right) engine models, including installation drag elements (greyed out data do not meet thrust requirements)

For the optimized quad jet engine, the cruise operating conditions are now very close to the Top of Climb design condition, resulting in a much better matching of engine air demand and intake flow. As a consequence, the installed SFC in the most relevant operating conditions Top of Climb and Mid Cruise, as well as during the transonic acceleration phase (TA) has significantly improved over the preliminary engine model. Also, the thrust requirements in the transonic acceleration phase are easily achieved with this new design (greyed-out data in the initial design would not achieve the respective thrust requirements due to high installation drag, red numbers are too high/low to meet overall flight performance goals).
The changed Top of Climb design condition results in a slightly lower OPR of the engine model, which is determined by the compressor exit temperature limitation. This in turn results in reduced applicable OPR-dependent emission limits, which is particularly relevant for NO_X emissions. The implications of this reduction are explained in more detail in the emissions modelling section.

3.5 Geometrical Engine Outline and Weight Estimation

After the design studies had been completed and a final engine design was selected, a methodology implemented in GTlab was applied to estimate the geometry and mass of the engine. This methodology consists of semi-empirical correlations based on existing aircraft engines.

3.5.1 Geometry Estimation

In a simplified description, the geometry estimation process transfers dimensionless annulus geometries of specific components (such as fan, compressor, turbine) to the components of the thermodynamic simulation model by using dimensionless geometry parameters, such as Mach numbers and hub-to-tip ratios. This so-called knowledge-based sketching method is an effective way of generating initial engine geometries in the preliminary design process. The geometry model is then checked with regard to the selected parameters and the engine model is adjusted if necessary. A detailed description of the process used here is described in [5].

The procedure described above was applied based on a Rolls Royce general arrangement published in [12]. This engine model was designed for a similar, smaller application (30 passenger supersonic airliner, cruise Mach number 1.6). The resulting flow path of the final geometry model is presented in Figure 5.

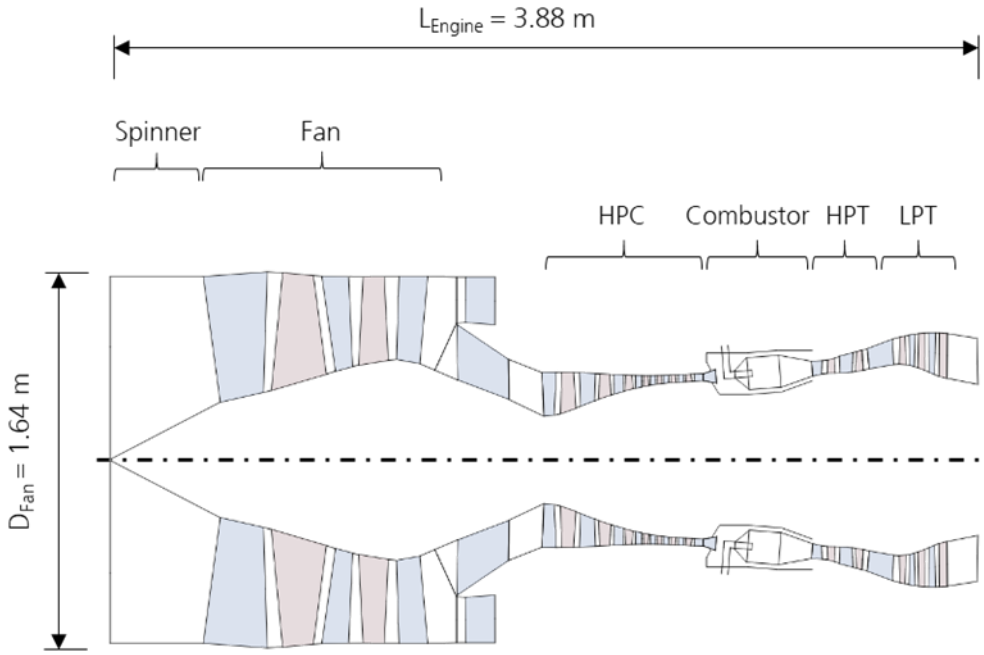

Figure 5 – Flow Flow path of final engine model as result of the geometry estimation tool (GTlab Sketchpad)

3.5.2 Mass estimation

Using the engine geometry model and the predetermined thermodynamic model, further correlations can be applied to estimate the engine weight excluding mixer, bypass channel and nozzle. These are expected to contribute only a small part of the total weight (<5%). The engine bare weight was estimated to be 4596kg using the procedures described in [5]. The engine weight and external dimensions are summarized in Table 3.

Bare engine weight (except mixer, bypass duct & nozzle) [kg]	4596
Engine length (Spinner to LPT) [m]	3.88
Fan diameter [m]	1.64
Center of gravity (starting at spinner entry) [m]	2.65

Table 3 – Weight and external dimensions of the final optimized engine model for the SENECA Ma 1.8 airliner

Compared to the previous design intended for a twinjet configuration, the final engine size and weight was reduced by approximately 30%. As a consequence, the total weight of all engines of the final, four-engine airliner design will be about 40% higher than that of the twinjet configuration. However, this weight increase is more than outbalanced by the better cruise fuel consumption of the final engine design.

4. Emissions Estimation

4.1 Introduction and Methods Applied

As an input to the emissions work package (WP4) of the SENECA project, an estimation of LTO-cycle emissions of the engine cycle presented herein has been performed. For this estimation, a procedure has been used based on established emission correlation methods, emissions data from reference engines and thermodynamic data from generic, DLR-owned engine models [10]. The reference emissions data has been taken from ICAO's Engine Emissions database (EEdb), version 29B [6]. Emission models for Nitrous Oxides (NO_X), unburned Hydrocarbons (HC), Carbon Monoxide (CO) as well as mass and number of non-volatile particles (nvPM) have been created. Correlation methods applied have been the P3-T3 method for NO_X [8], Omega methods for HC and CO [2] and

the DLR-created Döpelheuer method for nvPM mass [3]. No nvPM number method has been established so far, but an engine-specific estimation based on the geometric mean particle diameter (GMD) has been applied for the purpose of this deliverable.

As a general comment it should be considered that transferring the emissions behavior of one engine combustor to the engine cycle data of another engine is beyond the originally intended scope of application of these methods. However, with no other data or more reliable, simple estimation methods available, the application of these methods seems appropriate for this purpose. Nevertheless, the data presented herein should be regarded more as a scenario than as a prediction.

4.2 Reference Engine Emissions Data

The reference data required for the application of the correlation methods were taken from engines with somewhat similar properties to the final optimized Ma 1.8 airliner engine presented herein. The CFM56-7B (Tech Insertion combustor) has been selected as a reference engine, because the OPR and T3 values of DLR's generic model of this type are similar to those of the Ma 1.8 airliner engine. For comparison and consistency checks, also the Trent XWB series (Phase5 Tiled combustor) has been selected as a second reference.

All comparisons with existing engine types in the following sections refer to data from the respective DLR generic engine models.

4.3 Engine Emissions Certification Test Cycle

The emission indices of the reference engines are given in the ICAO EEdb for a standardized Landing and Take-off (LTO-) cycle as defined in Annex 16, Vol. II, Part III, Ch. 2 of the Convention on International Civil Aviation for subsonic applications. An LTO-cycle for supersonic engines is defined in Ch. 3 of the same document, however, this cycle is considered outdated and no longer applicable for new certifications. An updated LTO-cycle for SST emissions modelling purposes has been proposed by ICCAIA (International Coordinating Council of Aerospace Industries Associations) to the members of the SENECA project and has been brought forward to ICAO CAEP's Working Group 3. This cycle is similar to the subsonic one, but with reduced thrust setting and time in mode for the Climb condition as well as slightly increased Taxi/Idle thrust, to be more relevant to the operation of future supersonic, non-afterburning engines (Table 4):

	RRD-proposed supersonic LTO-cycle			
	Takeoff	**Climb out**	**Approach**	**Idle**
Rel. thrust (ISA SLS)	100%	65%	30%	10%
Time in mode [min]	0.7	2.0	4.0	26

Table 4 – Supersonic LTO-cycle proposed for use in SENECA by CAEP WG3

This cycle has been applied here for the emissions estimation and the results have been compared to the currently applicable limits of the subsonic emissions standards (CAEP/8 for NO_X, CAEP/2 for CO and HC, CAEP/11 new type (NT) for nvPM mass and number), as no updated limits for supersonic engines are available at this point in time.

The emissions metric to be compared against the applicable limit is the total mass of emissions, deposited in the LTO-cycle (Dp), divided by the maximum certified sea level static thrust (F_{00} = 100% LTO-cycle thrust). This metric Dp/F_{00} is multiplied by a characteristic factor, which is dependent on the number of engines measured, to account for statistical variations between individual engines. For this exercise, factors for 1 and 3 engines measured have been applied. The resulting metric values are referred to as C1 and C3 values, respectively.

4.4 Definition of Maximum Sea Level Static Thrust

The thrust levels of the LTO-cycle are defined as percentages of the maximum certified sea level static thrust, F_{00}. For subsonic engines, this parameter is determined by the engine technical limits like maximum allowable material temperatures at the combustor and/or compressor exit, which are present at the maximum take-off condition only.

In contrast, in supersonic engines the maximum temperatures are reached in supersonic flight. The take-off thrust, required by the airframe is far from reaching those temperature limits. Therefore, there is some ambiguity about the appropriate value of F_{00}. For this study, F_{00} was set to the engine thrust achieved in sea level static standard day conditions with an aerodynamic fan speed of 100%, which is 146.2kN. The minimum take-off thrust requirements are significantly below this value, however, it is assumed that potentially higher thrust may be applied initially, in order to enable reduced noise departure profiles by activating a variable noise reduction system (VNRS, also Programmed Lapse Rate, PLR) after lift-off.

4.5 Emissions Model Results

The results of the P3-T3 NO_X emissions model, based on the two reference engines are shown in Fig. 6 for both, subsonic (Ch. 2) and proposed new supersonic LTO-cycles. Also included are the reference emissions data of all thrust variants of the CFM56-7B and Trent XWB engine types,

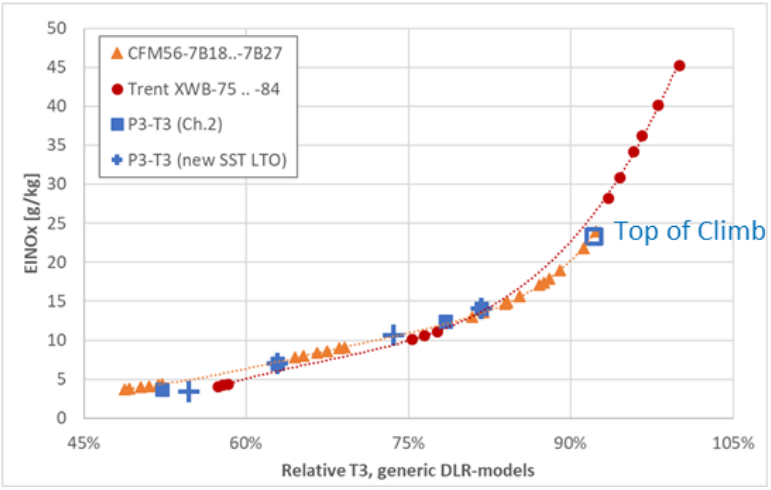

Figure 6 – LTO-cycle emissions data of reference engines and P3T3-modeled supersonic engine, against relative T3 of the generic DLR engine models, for both subsonic (Ch.2) and proposed new supersonic LTO cycles

Although the refence engines are of quite different size and technology, their emissions curves are similar when plotted against the relative (estimated) T3. The figure clearly shows that the combustor operating conditions of the supersonic engine in the LTO-cycle are significantly below the peak values of the subsonic references. Only the supersonic Top of Climb condition reaches the peak value of the CFM56-7B.

This example reveals a significant challenge in modeling full flight emissions of a supersonic aircraft: Since the correlation methods commonly used for this purpose rely on LTO-cycle emissions data only, significant extrapolation of this data would be required to estimate supersonic cruise emissions. This creates a potential source of large error, unless additional, high-power emissions data are available to guide the extrapolation.

High confidence was achieved in the prediction methods for the emission indices. By comparing non-proprietary DLR P3T3 and independently RRD proprietary correlations a very good agreement could be shown (Figure 7). Not forgetting the low technology readiness level (TRL) of this overall engine performance and emissions assessment, the non-proprietary emissions prediction results can be used for a wider range of applications and results can be easier published.

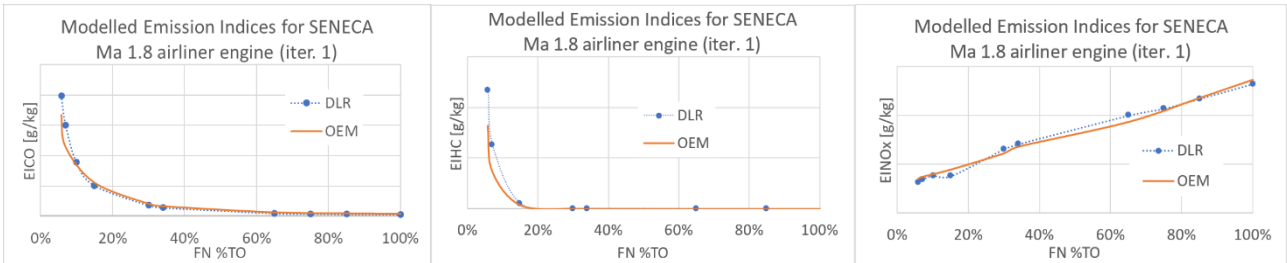

Figure 7 – Very good agreement found for DLR and independent OEM (RRD) prediction of EICO, EIHC and EINOx at SENECA Ma 1.8 cycle conditions for ICAO LTO computations.

Table 5 shows the modeled NO_X emissions indices (g NO_X per kg fuel) of the supersonic engine in the proposed supersonic LTO-cycle for both sets of reference data, together with the relative margin to the current subsonic limit (CAEP/8) for C1- and C3-corrected values of the metric Dp NO_X/F_{00}.

Emissions reference	EINOx [g/kg], by P3T3-correlation				% of CAEP/8 limit	
	Takeoff	Climb out	Approach	Idle	C1	C3
Trent XWB	16.53	11.87	7.60	3.85	114.3%	104.4%
CFM56-7B	14.04	10.61	6.98	3.35	100.7%	92.0%
Rel. Thrust	100%	65%	30%	10%		
Fuel [kg/s]	1.91	1.15	0.50	0.24		
Time [min]	0.7	2.0	4	26		

Table 5 – Modelled LTO-cycle NO_X emissions data for the final optimized Ma 1.8 airliner engine

The results for the two -quite different- reference engines turn out rather similar, building some confidence in the method applied here. It becomes obvious from these results that the subsonic CAEP/8 NO_X limit is hard to meet for this supersonic engine model. One reason is the low OPR of the engine at the maximum take-off condition, which is only 20.5, compared to 29.0 for the highest CFM56-7B thrust variant or even 41.1 for the Trent XWB-84. As the CAEP/8 NO_X limit is defined as a function of the OPR, this becomes particularly challenging for new supersonic engines with low OPR, similar to older technology subsonic engines, but high combustor temperatures according to the assumption of latest technology level.

An engine manufacturer would likely aim for a better margin to the limit, also for the characteristic C1 value. Probably there are trade-offs between NO_X and CO/HC which could be adjusted to improve the LTO NO_X performance, however, modelling such trade-offs is beyond the capabilities of the methods applied in this work.

HC and CO emissions resulting from the application of an Omega correlation with the CFM56-7B reference engine data are shown in Table 6 (relative thrust, fuel flow and time in mode are the same as in Table 5).

Emissions reference	EIHC [g/kg], by Omega-correlation				% of CAEP/2 limit	
	Takeoff	Climb out	Approach	Idle	C1	C3
CFM56-7B	0.03	0.04	0.08	0.64	13.7%	10.4%

Emissions reference	EICO [g/kg], by Omega-correlation				% of CAEP/2 limit	
	Takeoff	Climb out	Approach	Idle	C1	C3
CFM56-7B	0.86	1.74	5.55	19.91	59.3%	52.2%

Table 6 – Modelled LTO-cycle HC and CO emissions data for the final optimized Ma 1.8 airliner engine

The results indicate that there is still some margin available against the CO limit for potential trade-offs with NO_X, as described above. Higher CO emissions would indicate reduced low-power combustion efficiency and hence higher fuel consumption, but since the cruise thrust is well above the LTO-cycle points, in the low CO segment of the curve, this would probably not have a significant effect on the mission fuel burn.

Results of the nvPM mass and number models have been calculated as average values of the two reference engines, because they are significantly different in emissions levels and shape of the emission vs. thrust curve. These results are provided in Table 7.

nvPM EIs	nvPM model, based on average emission curves				% of CAEP/11 NT limit	
	Takeoff	Climb out	Approach	Idle	C1	C3
EIM [mg/kg]	73.85	36.36	14.42	6.62	59.8%	48.6%
EIN [1/kg]	6.17E+14	6.14E+14	5.27E+14	2.43E+14	88.4%	71.8%

Table 7 – Modelled LTO-cycle nvPM mass and number emissions data for the final optimized Ma 1.8 airliner engine

There is still a lot of uncertainties in nvPM measurements and modelling, and also large variations between different engine types. However, these results are within the range of existing products and therefore expected to provide a realistic starting point for the assessment of environmental impacts from supersonic airliners.

5. Summary and Conclusions

An engine cycle for a supersonic airliner application with a design Mach number of 1.8 has been designed in an iterative manner, taking into account multiple objectives like engine efficiency, lifetime and installation drag as well as noise and emission performance.

The result of this work and the process itself has revealed numerous and sometimes challenging differences to the design process for subsonic engines. Similar to fuel efficiency, which is important for the range and the commercial viability of the final product, also noise and emissions requirements turned out highly challenging. The final engine model, resulting from the design and optimization process presented herein, is expected to meet all these requirements, although with sometimes low margin and some inherent uncertainties, resulting from the more academic nature of the tools and methods applied.

The results of this work have been provided to the SENECA project's noise and emissions modeling work packages and will be used as inputs for further assessment of the local and global environmental impact of newly designed supersonic aircraft.

6. Copyright Statement

References

[1] Berton, J. J.: *A Comparative Propulsion System Analysis for High-Speed Civil Transport*, NASA TM 2005-213414, NASA, 2005

[2] Deidewig, F., Döpelheuer, A., Lecht, M.: *Methods to Assess Aircraft Engine Emissions in Flight*, ICAS-96-4.1.2, 1996

[3] Döpelheuer, A.: *Anwendungsorientierte Verfahren zur Bestimmung von CO, HC und Ruß aus Luftfahrttriebwerken*, DLR Research Report FB-2002-10, Institute of Propulsion Technology, DLR, Köln, 2002

[4] Grieb, H.: *Projektierung von Turboflugtriebwerken*, ISBN 3-7643-6023-2, Birkhäuser Verlag, Basel, 2004

[5] Häßy, J.: *Knowledge-Based Conceptual Design Methods for Geometry and Mass Estimation of Rubber Aero Engines*, ICAS 2022, Stockholm 2022, Paper submitted

[6] ICAO: *Engine Emissions Databank*, https://www.easa.europa.eu/domains/environment/icao-aircraft-engine-emissions-databank, version 28C, accessed Juli 2021

[7] Kowalski, E. J.: *A Computer Code for Estimating Installed Performance of Aircraft Gas Turbine Engines – Vol.3 Library of Nozzle/Inlet Configurations and Performance Maps*, 1979, NASA Report NASA/CR-159693

[8] Madden, P., Park, K., *Methodology for Predicting NOx Emissions at Altitude Conditions from Ground Level Engine Emissions and Performance Test Information*, Rolls Royce Technical Report No DNS 90713, April 2003

[9] Mattingly, J.D., Heiser, W.H., Pratt, D.T., Boyer, K.M., Haven, B.A.: *Aircraft Engine Design*, 3rd edition, 2018

[10] Otten, T., Plohr, M., von der Bank, R.: *Gegenüberstellung des Emissions-Verbesserungspotentials von Brennkammertechnologien und anderen Weiterentwicklungen am Lufttransportsystem*, DGLR Jahrbuch 2006 (131), Seiten 597-606, Deutscher Luft- und Raumfahrtkongress 2006, 2006-11-06 - 2006-11-09, Braunschweig, ISSN 0070-4083

[11] Reitenbach, S., Vieweg, M., Becker, R., Hollmann, C., Wolters, F., Schmeink, J., Otten, T., Siggel, M.: *Collaborative Aircraft Engine Preliminary Design using a Virtual Engine Platform, Part A: Architecture and Methodology*, in: AIAA Scitech 2020 Forum, AIAA SciTech Forum 2020, 06.-10. Jan. 2020, Orlando, USA, ISBN 978-162410595-1, 2020

[12] Welge, H.R., et al.: *N+2 Supersonic Concept Development and Systems Integration*, 2010, NASA Report NASA/CR-2010-216842